SIMULATING PROTON SYNCHROTRON RADIATION IN THE ARCS OF THE LHC, HL-LHC, AND FCC-hh*

Gerardo Guillermo Canton[†‡], CINVESTAV, Merida, Mexico;
David Sagan, Cornell U., Ithaca, New York, U.S.A.;
Frank Zimmermann, CERN, Geneva, Switzerland

Abstract

At high proton-beam energies, beam-induced synchrotron radiation is an important source of heating, of beam-related vacuum pressure increase, and of primary photoelectrons, which can give rise to an electron cloud. We use the Synrad3D code developed at Cornell to simulate the photon distributions in the arcs of the LHC, HL-LHC, and FCC-hh. Specifically, for the LHC we study the effect of the "sawtooth" chamber, for the HL-LHC the consequences of the ATS optics with large beta beating in the arcs, and for the FCC-hh the effect of a novel beam-screen design, with a long slit surrounded by a "folded" antechamber.

INTRODUCTION

The simulation code Synrad3D developed at Cornell [1] generates and tracks synchrotron radiation photons in an accelerator beam line and includes both specular and diffuse reflection on the chamber surface. The photons are generated randomly at any point in the lattice with a distribution appropriate for the local bending radius. Non-zero beam orbits are accommodated. When a photon hits the chamber wall the reflection probability depends on the energy and angle of incidence, as well as the material (with the possibility of multiple layers), and its surface roughness. As one option, reflection tables provided by the LBNL Center for X-Ray Optics [2] can be employed. The simulations discussed in the following will make use of these tables. In the simulations the photon energies are generated with a lower cut off at 4 eV, i.e., only photons with higher energies are considered, as these higher-energetic photons may generate photoelectrons or degrade the vacuum. Initial LHC simulations with Synrad3D were reported in Ref. [3].

LHC SAWTOOTH

A 7 TeV protom beam passing through the 8.33 T dipole field of the LHC arcs has a photon critical energy of about 44 eV. In the LHC cold arcs, the synchrotron radiation is intercepted by a beam screen at a temperature of 5–20 K which is higher than the 1.9 K of the cold bore [4]. The

beam screen is made of stainless steel with a 75 μm copper coating. The total thickness of the beam screen is 1.08 mm including the copper [5].

Example reflection probabilities for an LHC like chamber surface with a 10 nm thick carbon layer on top of copper with a surface roughness of 200 nm are presented in Fig. 1. The carbon layer models the effect of surface conditioning due to electron bombardment ("electron-cloud scrubbing") [6].
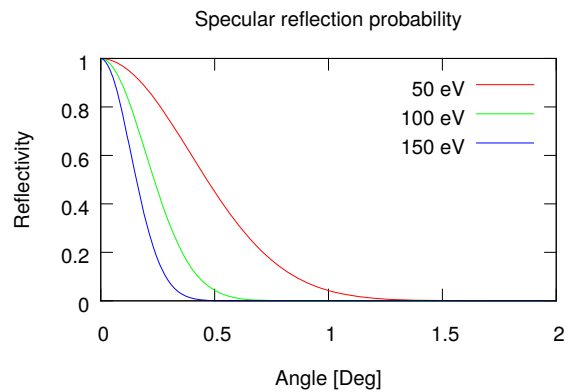

Figure 1: Photon reflectivity as a function of angle of incidence for several different photon energies, considering a 10 nm carbon layer on top of a copper surface with 200 nm roughness.

To reduce photon reflections, the inner surface of the beam screen, on the outward side, features a sawtooth pattern, which should ensure almost perpendicular impact. The sawtooth pattern has a longitudinal period of about 500 μm and a horizontal amplitude of 40 ± 20 μm [7]. The vertical extent of the sawtooth pattern is ±7.5 mm from the equatorial plane [5]. Figure 2 shows the model of the LHC sawtooth beam screen implemented in Synrad3D.

Simulated distributions of absorbed photons with and without the sawtooth are shown in Fig. 3 and the corresponding reflection distributions in Fig. 4. With the sawtooth present, only 2% of the photons are absorbed on each of the top and bottom surfaces, whereas 48% are absorbed on either of the two sides. By contrast, with no sawtooth, about 43% of the photons are absorbed on the primary impact side, 24% on the opposite side, and 16–17% each on the top and bottom of the chamber.

These results, in particular the change in the azimuthal distribution due to the sawtooth surface, are roughly con-
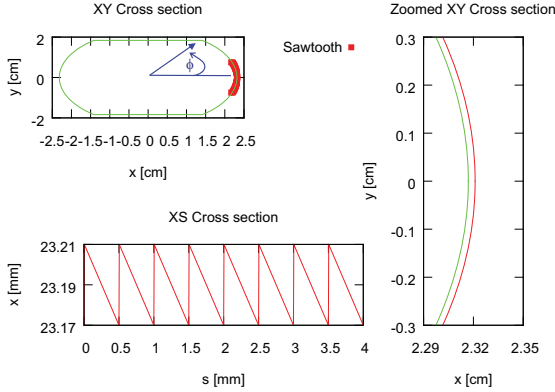
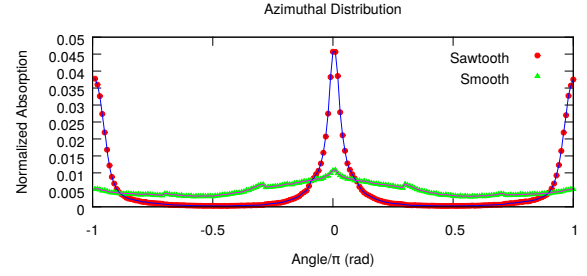Figure 2: Synrad3D model of LHC beam screen design with sawtooth, and definition of azimuthal angle ϕ.

Figure 3: Simulated azimuthal distribution of finally absorbed photons without and with sawtooth chamber, normalized as fraction of the total with an angular bin size $\pi/100$. The azimuthal angle ϕ is the angle measured from the center of the chamber with respect to the horizontal (outward direction), as indicated in Fig. 2.

sistent with experimental measurements in open set ups (i.e., with a limited length of test chamber) at VEPP-2M [8, 9, 10] and ELETTRA [11].

Also a quantitative comparison is possible. For example, the VEPP-2M measurements for a smooth copper-coated chamber without sawtooth at 20 mrad grazing incidence revealed a photon forward reflectivity R of up to 95% [9], This would correspond to an average number of $n_{\mathrm{pass}} = 1/(1 - R) \approx 20$ photon passages through the chamber until absorption. Adding another 2–4% diffusely reflected photons [9], the average number of photon passages in the measurements would be between 33 and 100, which is consistent with the value of about 80 found by the Synrad3D simulations, in the top picture of Fig. 4. For the sawtooth surface a much lower total reflectivity of about 10% was measured [11]. This translates into an average number of passages not much above 1, while the Synrad3 simulations predict a value below 3 (see the bottom picture of Fig. 4).

The almost 10-fold reduction of photons hitting the top and bottom of the chamber confirms the intended effect of the sawtooth structure, that is, to greatly decrease the number of photoelectrons generated above and below the beam in the arc dipole magnets, where, following the vertical field lines, they could approach the beam and contribute to further electron-cloud build up.

HL-LHC

The HL-LHC has nearly twice the beam current of the LHC, which will approximately double the photon flux. In the arcs, a second main difference between the LHC [4] and the HL-LHC [12] is a beta wave introduced through the long adjacent arcs in order to squeeze the β^* at the two high-luminosity collision points. This optics scheme is called the achromatic telescopic squeeze (ATS) [13]. It exists in round ($\beta_x^* = \beta_y^*$) and flat configurations ($\beta_x^* \gg \beta_y^*$ in one IP, and $\beta_x^* \ll \beta_y^*$ in the other). With a large vertical beta beat in the arcs 45 and 56, the distribution of pho-
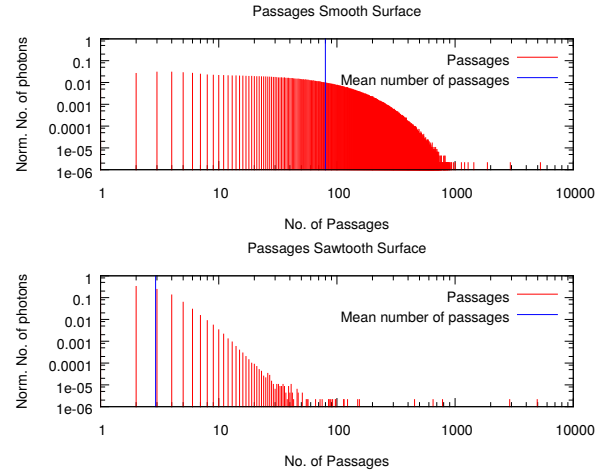

Figure 4: Distribution of number of photon passages till absorption (equal to the number of true reflections plus one) without (top) and with sawtooth chamber (bottom).

tons hitting the chamber wall (and being absorbed there) may change. For example, in the "pre-squeeze" optics with $\beta_{x,y}^* = 0.44$ m, the minimum beta function in the arc is around 32 m, whereas for a non-baseline flat ATS optics, with $\beta_y^* = 0.05$ m in IP5, the minimum vertical beta function shrinks to $\beta_{y,\mathrm{min}} \approx 16$ m in arcs 45 and 56. (In the baseline flat ATS optics the vertical beta function in IP5 is 0.075 m.) Nevertheless, considering the nominal geometric rms emittance, ϵ_y, of about 0.3 nm the corresponding maximum rms divergence of $\sigma_{y',\mathrm{max}} \approx (\epsilon_y/\beta_{y,\mathrm{min}})^{1/2} \approx 5 \times 10^{-6}$ is still much smaller than the rms angle of the photon emission, $\sim 1/\gamma \approx 1.3 \times 10^{-4}$. Therefore, no large effect of the ATS optics on the photon distribution is expected. This expectation is confirmed by Synrad3D simulations (see Fig. 5), in which we compare photon distributions for a squeezed flat optics with those for the HL-LHC "pre-sequeeze" (equal to the standard LHC arc optics).
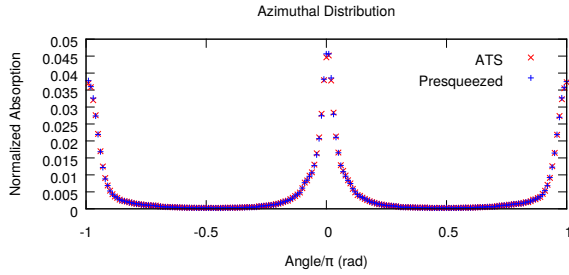
Figure 5: Azimuthal photon distribution without ($\beta_x^* = 0.44$ m, $\beta_y^* = 0.44$ m) and with a flat ATS optics ($\beta_x^* = 0.2$ m, $\beta_y^* = 0.05$ m), considering the nominal HL-LHC emittance ($\epsilon_y = 0.3$ nm, rms). The vertical axis corresponds to fraction of the total with an angular bin size $\pi/100$.

FCC-hh

The FCC-hh will feature novel beam-screen shapes with an integrated compact antechamber, as is illustrated in Fig. 6. Slots in the equatorial plane with a vertical full height of 3 mm will absorb most of the photons, thereby facilitating the beam-screen cooling and stabilizing the beam vacuum [14, 15].

The simulated photon distribution for the FCC-hh is illustrated in Fig. 7. For a centered orbit, a fraction of 0.6% of the emitted photons is hitting the beam screen outside of the absorber slots. Figure 8 shows the dependence of this fraction on a vertical orbit offset, setting a tolerance on the acceptable closed-orbit distortions in the FCC-hh of about 1 mm (peak offset from horizontal plane).
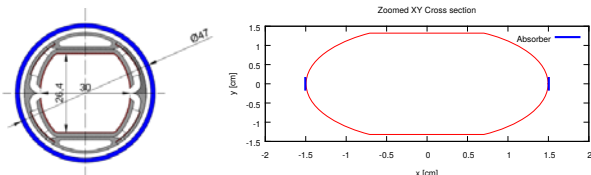
Figure 6: FCC-hh beam-screen design with integrated "folded" antechamber; design by R. Kersevan [14, 15] (left) and simplified model used in Synrad3D where antechamber slots are represented as perfect absorbers (right). [14].

CONCLUSIONS

Simulations of photon reflection and absorption with Synrad3D confirm the expected positive effects of the beam-screen sawtooth surface on the synchrotron radiation for the LHC and of the novel beam-screen shape for the FCC-hh. They also confirm that the ATS optics does not change the photon distribution for the HL-LHC arcs. Finally they suggest an orbit tolerance for the FCC-hh.
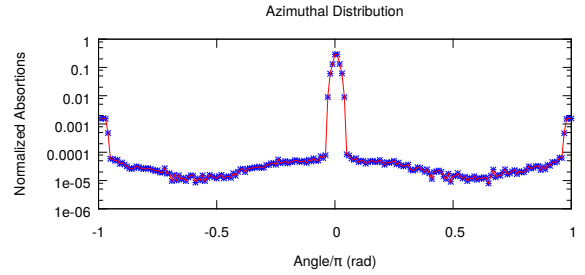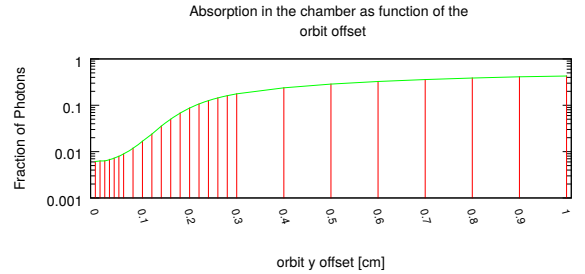

Figure 7: Azimuthal distribution of photons absorbed on the inner beam screen surface, for the FCC-hh chamber design of Fig. 6. The vertical axis corresponds to fraction of the total with an angular bin size $\pi/100$.

Figure 8: Simulated fraction of photons absorbed on the inner FCC-hh beam screen as as function of peak vertical orbit error, for the FCC-hh chamber design of Fig. 6.

ACKNOWLEDGMENTS

REFERENCES

[1] G. Dugan, D. Sagan, "Synrad3D photon propagation and scattering simulations", Proc. Joint INFN-CERN-EuCARD-AccNet Workshop on Electron-Cloud Effects, La Biodola, Isola d'Elba, Italy, 5 — 9 June 2012, pp. 117–129, CERN-2013-002.

[2] LBNL Center for X-Ray Optics, http://henke.lbl.gov/optical_constants/

[3] G.H.I. Maury Cuna, D. Sagan, G. Dugan, "Synchrotron-Radiation Photon Distribution for Highest Energy Circular Colliders", Proc. 4th International Particle Accelerator Conference, Shanghai, China, 12–17 May 2013, pp. 1340, CERN-ACC-2013-0128,

[4] O. Brüning et al., "LHC Design Report, Volume v.1: the LHC Main Ring", CERN-2004-003-V-1 (2004).

[5] V. Baglin, private communication, 14 December 2015.

[6] R. Cimino et al., "Nature of the Decrease of the Secondary-Electron Yield by Electron Bombardment and its Energy Dependence", Phys. Rev. Lett. 109, 064801 (2012).

[7] LHC Technical Drawing `LHCVSSB_0037-vAB dipole.plt`.

[8] V.V. Anashin et al., "Azimuthal Distribution of Photoelectrons for an LHC Beam Screen Prototype in a Magnetic Field", CERN Vacuum Technical Note 99-06 (1999).

[9] V.V. Anashin et al., "Reflection of Photons and Azimuthal Distribution of Photoelectrons in a Cylindrical Beam Pipe", LHC Project Report 266 (1999).

[10] V.V. Anashin et al., "Magnetic and Electric Field Effects on the Photoelevtron Emission from Prototype Emission from Prototype LHC Beam Screen Material", Vacuum 60 (2001) 255–260.

[11] N. Mahne et al., "Photon Reflectivity Distributions from the LHC Beam Screen and Their Impplications on the Arc Beam Vacuum System", Applied Surface Science 235 (2004) 221–226.

[12] G. Apollinari et al., "High-Luminosity Large Hadron Collider (HL-LHC): Preliminary Design Report", CERN-2015-005.

[13] S. Fartoukh. "Achromatic telescopic squeezing scheme and application to the LHC and its luminosity upgrade", Phys. Rev. ST Accel. Beams 16 (2013) 11, 111002.

[14] R. Kersevan, "Beam Screen Design and Cooling, Vacuum Aspects, Synchrotron Radiation", Review of the FCC-hh Injection Energy, CERN, 16 October 2015, `http://indico.cern.ch/event/449449`.

[15] R. Kersevan, "FCC-hh Double-Slot Beam Screen; Density Profiles vs Slot Size, Misalignments, and Magnet Temperature", CERN, 26 November 2015.